

Low-Field de Haas-van Alphen Study of the Fermi Surface of Aluminum*†

C. O. LARSON‡ AND W. L. GORDON

Department of Physics, Case Institute of Technology, Cleveland, Ohio

(Received 26 September 1966)

The third-zone Fermi surface of aluminum has been studied using the low-field de Haas-van Alphen effect. The observed de Haas-van Alphen periods have been assigned to the principal portions of the third-zone surface according to the model proposed by Ashcroft. Several cyclotron masses have been determined and are found to be consistent with cyclotron resonance results, where comparison is possible. de Haas-van Alphen cyclotron masses have been compared with the band-structure masses calculated by Ashcroft. This comparison indicates that, within the uncertainties in observed and calculated masses, there is a 30 to 50% enhancement of the band-structure masses over the third-zone surface, in agreement with the calculations of Ashcroft and Wilkins.

INTRODUCTION

THE de Haas-van Alphen (dHvA) oscillations in the magnetic susceptibility, periodic in $1/H$ with frequency proportional to an extremal cross section of the Fermi surface, provide a powerful tool for the study of the Fermi surface of metals. According to Onsager,¹ and Lifshitz and Kosevich,² the period of the oscillation is related to the extremal cross section S_m (in k space) through the expression

$$P = 2\pi e / \hbar c S_m = 9.55 \times 10^{-9} / S_m \text{ (in } \text{\AA}^{-2}\text{)}.$$

This dHvA study of aluminum was initiated to explore the details of the third-zone portion of the Fermi surface. Several models have been proposed for this surface beginning with Harrison's³ nearly-free-electron model which was very successful in fitting the general features of Gunnensen's⁴ early dHvA results. This model was modified by Harrison⁵ using four orthogonalized plane waves (OPW) along with Heine's⁶ band-structure calculations, and in a similar manner by Segall⁷ using his own band-structure calculations. More recently, Ashcroft⁸ carried out a four OPW calculation adjusted to fit two observed⁴ extremal cross sections of the third-zone surface. His results differ from the previous models in several important details which are precisely those required to yield an excellent fit with the experimental data.

The first systematic dHvA study in aluminum was carried out by Gunnensen⁴ in fields up to 15.4 kG. He

observed two distinct classes of dHvA periods which he termed, appropriately, high frequency (HF) and low frequency (LF) since they differed in frequency by approximately a factor of 10. He was able to determine the angular dependence of the HF periods fairly completely but was able to determine the LF periods only at major symmetry directions. Gunnensen's resolution was limited by the fact that he plotted the torque point by point.

In the present study, the torque exerted by the magnetic field on the specimen was plotted directly as a function of the reciprocal of the field by an automatic torque-recording circuit. This technique preserved the fine structure of the data and, in addition, provided a continuously varying function which is a necessity if filtering for a particular frequency component is to be done. The periods observed ranged from 1×10^{-7} to 40×10^{-7} G⁻¹. The angular dependence of these periods with respect to crystalline direction was determined and was found to be quite consistent with Ashcroft's predictions⁸ and in generally good agreement with the results of Volskii⁹ as obtained from the oscillatory surface resistance. We are unable to compare our data with the high-field data of Priestley¹⁰ since none of the oscillations arising from second-zone cross sections of the Fermi surface are observed in fields up to 23 kG in our apparatus.

The temperature dependence of the amplitude of the oscillations was studied in orientations where it could be determined, and several representative effective cyclotron masses were determined for both the HF and LF periods. Masses for the HF oscillations were found to be fairly consistent with those obtained by Moore and Spong¹¹ in their cyclotron resonance experiments. Masses corresponding to LF orbits are of particular interest because no reliable cyclotron resonance data are available as yet and because Ashcroft¹² has calcu-

* Supported by the Air Force Office of Scientific Research under Grant Nos. AFOSR 62-222 and 536-64.

† Submitted (by C.O.L.) in partial fulfillment of the requirements for the Ph.D. degree at the Case Institute of Technology.

‡ Present address: Department of Physics, Wisconsin State University, River Falls, Wisconsin.

¹ L. Onsager, *Phil. Mag.* **43**, 1006 (1952).

² I. M. Lifshitz and A. M. Kosevich, *Zh. Eksperim. i Teor. Fiz.* **29**, 730 (1955) [English transl.: *Soviet Phys.—JETP* **2**, 636 (1956)].

³ W. A. Harrison, *Phys. Rev.* **116**, 555 (1959).

⁴ E. M. Gunnensen, *Phil. Trans. Roy. Soc. (London)* **A249**, 299 (1957).

⁵ W. A. Harrison, *Phys. Rev.* **118**, 1182 (1960).

⁶ V. Heine, *Proc. Roy. Soc. (London)* **A240**, 340 (1957).

⁷ B. Segall, *Phys. Rev.* **124**, 1797 (1961); **131**, 121 (1963).

⁸ N. W. Ashcroft, *Phil. Mag.* **8**, 2055 (1963).

⁹ E. P. Volskii, *Zh. Eksperim. i Teor. Fiz.* **46**, 123 (1964) [English transl.: *Soviet Phys.—JETP* **19**, 89 (1964)].

¹⁰ M. Priestley, *Phil. Mag.* **7**, 1205 (1962).

¹¹ T. W. Moore and F. W. Spong, *Phys. Rev.* **125**, 846 (1962).

¹² N. W. Ashcroft, thesis, Cambridge University, 1964 (unpublished).

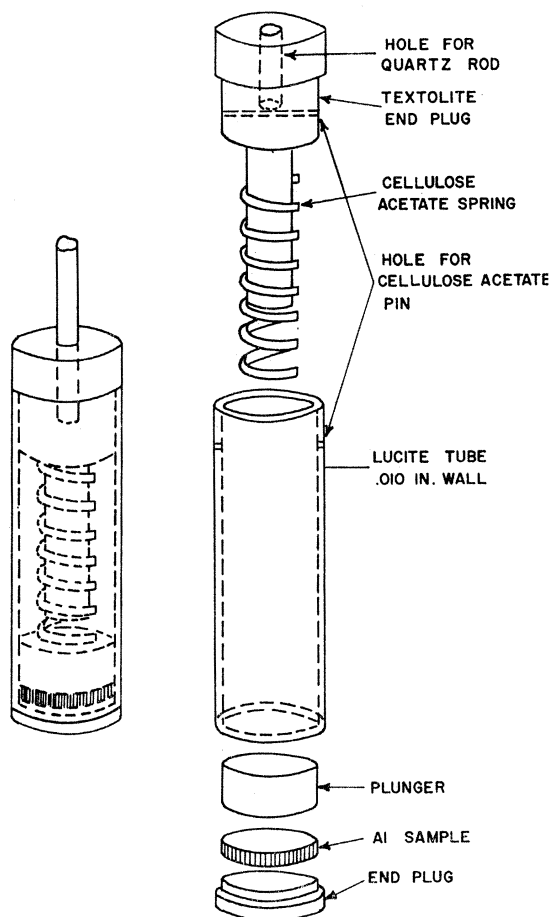


Fig. 1. The sample holder. The sample is pressed against the holder by the cellulose acetate spring and the cellulose acetate pin keeps the holder from rotating with respect to the quartz rod.

lated band-structure cyclotron masses at several symmetry directions for both LF and HF orbits. Furthermore, Ashcroft and Wilkins¹³ have recently estimated that enhancement by the electron-phonon interaction is sufficient to raise the measured cyclotron masses by a factor of 1.48 over the band-structure values in aluminum. Thus it was hoped that the comparison of the LF and HF masses to the calculated values might permit a test of the isotropy of the enhancement factor over the third-zone surface.

SAMPLE PREPARATION

The single crystals used in this experiment were grown from a boule of commercially prepared 99.9999%-purity aluminum having a residual resistance ratio of about 5000 in the region where the samples were cut.

The crystals were grown using the strain-anneal technique. The aluminum bar from which the sample was to be cut was given a critical strain of about

3-5%. An annealing furnace having a steep temperature gradient was then passed over the bar yielding large crystals from which samples could be cut. The crystals were oriented for cutting by using x-ray back-reflection Laue photographs. These photographs showed no signs of microstructure greater than 0.3° .

Since a spark cutting facility was not yet available, the samples were cut to the desired size and orientation by a string saw etching technique. Since acids do not readily attack aluminum, the etching solution was somewhat of a problem. A solution of cupric chloride in water was found to work quite well, the concentration not being too critical. The copper, deposited on the aluminum, was readily dissolved with nitric acid.

The final samples were cylinders about $\frac{3}{16}$ in. in diameter and $\frac{1}{32}$ in high with the cylinder axis oriented parallel to one of the major crystal symmetry directions. The disk shaped samples were mounted in a Lucite holder as shown in Fig. 1. The cellulose acetate spring was used to secure the sample since it was found that gluing the sample face directly to a holder introduced strain unless thermal expansions were matched closely.

EXPERIMENTAL PROCEDURE

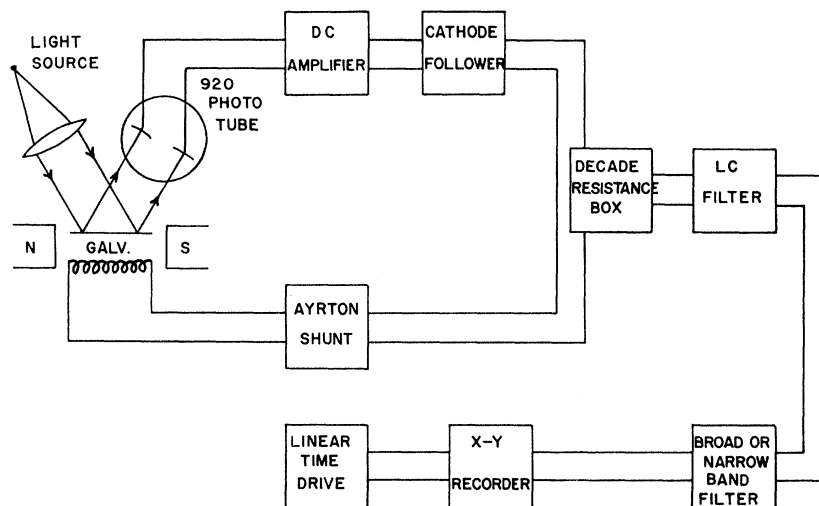
In this study, the dHvA oscillations were observed by recording the torque exerted by a magnetic field on the metal sample which was maintained at liquid-helium temperatures. A self-balancing torque magnetometer designed by Joseph and Gordon¹⁴ was used in conjunction with a metal cryostat of standard design for use in a magnetic field. The aluminum sample mounted as in Fig. 1 was suspended at the end of a long, straight, quartz rod which held it in the center of the uniform region of the magnetic field. The quartz rod and sample were enclosed in a glass tube which was filled, to a pressure of about 2.5 cm, with helium exchange gas and immersed in liquid helium. A 12-in. type 4012-3B Varian magnet was used to supply fields up to 23 kG. The magnet was rotatable about a vertical axis making possible all field directions in the horizontal plane. The low magneto-resistance of pure aluminum makes the problem of eddy currents a serious one if it is desired to sweep the magnetic field. To minimize the production of eddy currents, the samples were cut in the shape of wafer thin cylinders to present a very small amount of surface area perpendicular to the field direction.

In the magnetometer, Fig. 2, the dc amplifier produces a voltage which is approximately proportional to the angular deflection of the crystal and galvanometer coil from which it is suspended. This voltage (by means of the cathode follower) produces a feedback current through the galvanometer which depends on a series decade resistance and on a shunt setting.

¹³ N. W. Ashcroft and J. W. Wilkins, Phys. Letters 14, 285 (1965).

¹⁴ A. S. Joseph and W. L. Gordon, Phys. Rev. 126, 489 (1962).

FIG. 2. Schematic of the torque magnetometer and automatic recording circuit used to plot the torque directly as a function of time. The magnetic field is independently swept at such a rate that its reciprocal increases linearly in time.



Because the restoring torque due to the galvanometer suspension is negligible, this current is proportional to the torque exerted by the magnetic field on the sample. Thus the stiffness of the system depends on the fixed amplifier gain, on the value of the series resistance, and on the shunt setting so that it is adjustable, within limits, to control the range of the small angular deflections of the crystal.¹⁵ The signal across the decade resistance is filtered by a fixed *LC* network to remove high-frequency noise and then fed to the *y* side of a Moseley *x-y* recorder, either directly or through tunable broad or narrow passband filters.

To make selective filtering possible it is necessary that a given *dHvA* frequency have a constant value in time. Thus, since *dHvA* frequencies are periodic in $1/H$ it is necessary to sweep the magnetic field in such a way that its reciprocal increases linearly in time. This is accomplished by applying a time-varying sweep voltage to the magnet power supply. This voltage is obtained by a combination of gear-driven potentiometers and is described in detail in Ref. 16. When the *x* side of the *x-y* recorder is driven linearly in time, the trace displays torque on the sample as a function of the reciprocal of the magnetic field.

The magnetic field at the start and finish of a sweep was determined from the magnet current by monitoring the voltage drop across a series resistor made of manganin wire and immersed in an oil bath. Primary calibration was accomplished with a nuclear magnetic resonance probe. It was found that if the magnet current was brought to zero after completing a field sweep and

then was brought up to its maximum value for the next sweep, the field values were reproducible to within 0.2%.

The temperature of the sample was determined by measuring the helium vapor pressure in equilibrium with the bath. A Wallace and Tiernan absolute pressure gauge was used to measure the pressure. Tests performed using a carbon resistor indicated that the actual sample temperature was the same as that of the bath.

Near the completion of the study a few runs were made with the field modulation technique,¹⁷ working at a frequency of 100 cps. In this way, data were obtained for field directions along symmetry axes.

FILTERS

Since the number of frequencies present in a given orientation often numbered six or more, filters of two kinds were used. A broad passband filter was used when it was only desired to separate the high frequencies from the low frequencies. These frequencies differed by about a factor of 10 so a filter *Q* of 0.6 was adequate. The broad band filter employing a standard differentiator-integrator circuit with an operational amplifier was tunable and either differentiated or integrated the signal depending upon the values of the tuning resistance and capacitance.

To separate frequencies which differed by a factor of 2 or less it was necessary to use a narrow band filter having a *Q* of about 3. Ideally it would be advantageous to use the highest *Q* (narrowest passband) filter available. There are, however, practical limitations which restrict *Q*.

As the *Q* of a filter is increased, the decay time for filter transients also increases. This sets an upper limit on the maximum allowable *Q* since it must be low enough to allow filter transients to damp out before

¹⁵ Where *dHvA* periods vary slowly with angle, the magnitude of these angular deflections may be safely increased to raise their level above the angular deflections due to low-frequency noise vibrations. However, in the presence of a large-amplitude *dHvA* component, a second component whose frequency changes rapidly with angle will exhibit frequency modulation effects. Higgins [R. J. Higgins, J. A. Marcus, D. H. Whitmore, Phys. Rev. **137**, A1172 (1965)] has also observed this effect in his work on zinc.

¹⁶ C. O. Larson, thesis, Case Institute of Technology, 1965 (unpublished).

¹⁷ R. D. Plummer and W. L. Gordon, Phys. Rev. Letters **13**, 432 (1964).

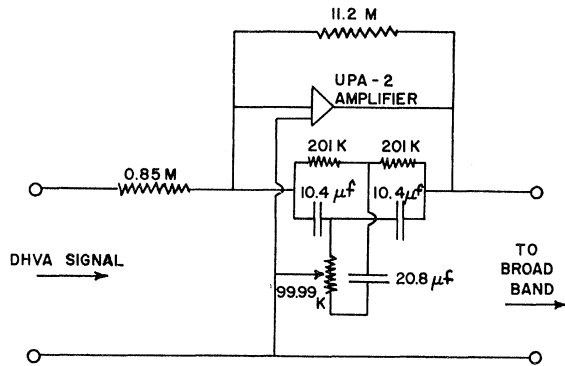


FIG. 3. The narrow passband filter circuit which employs a tunable twin-T filter in the feedback of an operational amplifier. This filter was used in series with a broad band filter.

reaching the field region over which data is to be taken. In addition, the linearity of the $1/H$ drive sets limits on the Q possible. Deviations in the $1/H$ drive result in a dHvA frequency which is not constant in time causing the frequency to ride up and down on the steeply peaked gain curve. The resulting fluctuations in amplitude, of course, become more important as the Q is increased. The $Q=3$ provided a compromise between resolution, filter ring, and $1/H$ drive irregularities.

The narrow band filter employed a tunable twin-T filter in the feedback circuit of an operational amplifier as illustrated in Fig. 3. With this feedback loop, the amplifier is highly degenerative at all frequencies except those near the twin-T null frequency where the over-all gain rises to a value proportional to the ratio of the feedback resistance to the input resistance. The analysis of such a filter, employing a nontunable twin-T, has been discussed by Hastings.¹⁸

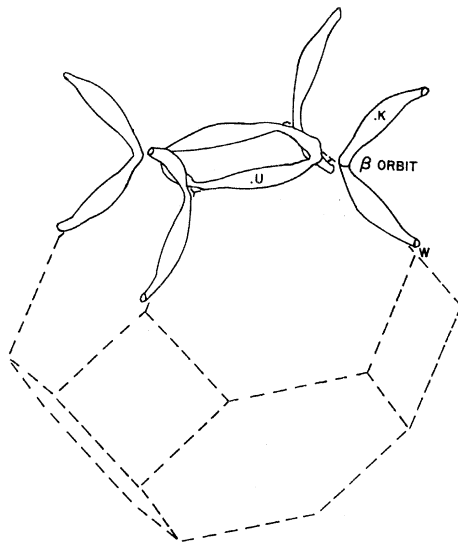


FIG. 4. Ashcroft's model (1) for the third-zone Fermi surface of aluminum in the reduced zone scheme. The principal symmetry points are labeled.

¹⁸ A. E. Hastings, Proc. IRE 34.3, 126P (1946).

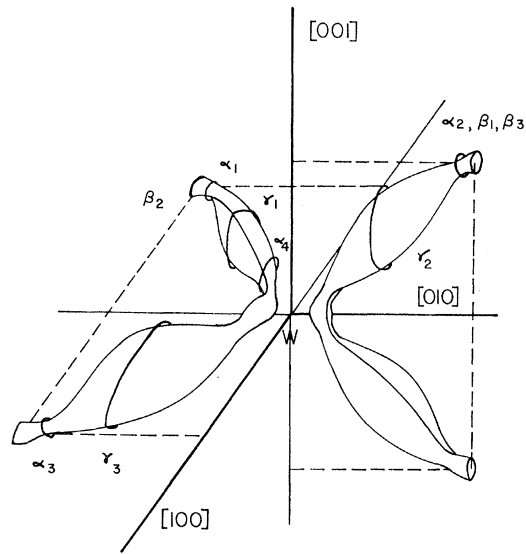


FIG. 5. An enlarged section of the third-zone Fermi surface of aluminum near the point W for Ashcroft's model (1) in the reduced zone scheme. With the exception of β_3 , the orbits shown correspond to the types of extremal cross sections observed with the field in the $[010]$ direction. The suspension is $[001]$.

The upper limit on the magnet sweep speed, determined by eddy currents and the noise frequency relative to the signal, forced the frequency range to be low. The resistance component of the twin-T could not be increased arbitrarily due to the stability requirement of the filter as discussed by Hastings,¹⁸ thus it was necessary to use the large capacitance values indi-

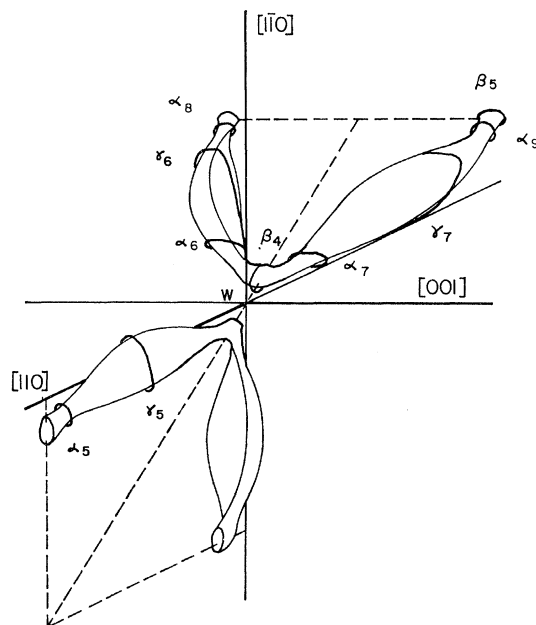


FIG. 6. An enlarged section of the third-zone Fermi surface of aluminum near the point W for Ashcroft's model (1) in the reduced zone scheme. With the exception of β_4 , the orbits shown correspond to the types of extremal cross sections observed with the field in the $[110]$ direction. The suspension is $[110]$.

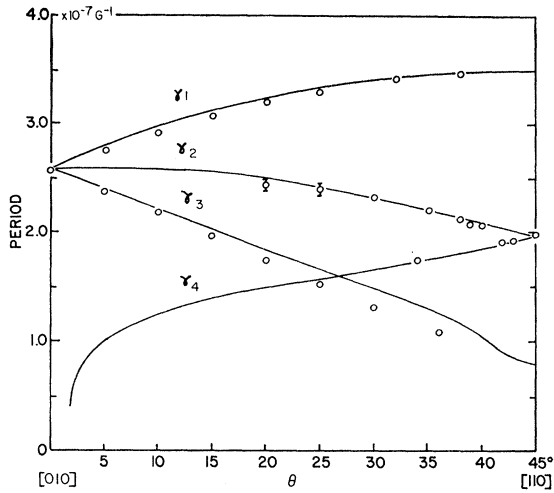


FIG. 7. The angular variation of the γ periods with θ for the (001) plane. In this and the three following figures, the angle θ is the angle between the field direction and a $\langle 100 \rangle$ direction, the \circ points are experimental data, and the solid lines follow Ashcroft's model. Uncertainties are about the size of the data circles except where indicated otherwise. The period branches are labeled to be consistent with the orbits shown in Fig. 5.

cated in Fig. 3. The dHvA periods were converted to a time scale by measuring the amount of time required to plot a given number of oscillations having a known period in G^{-1} . The filter could then be tuned to preferentially amplify any desired dHvA frequency component. The resolution obtained is discussed further in the data analysis section.

THE MODEL

Heine⁶ has shown that throughout most of the first and second zones of aluminum, the valence wave function can be represented as a single OPW. The agree-

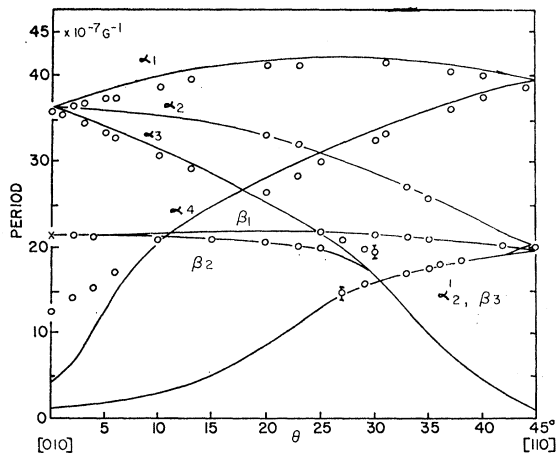


FIG. 8. The angular variation of the α and β periods for the (100) plane. In this and the two following figures, the point labeled \times was obtained by field-modulation methods. The period branches are labeled to be consistent with the orbits shown in Fig. 5.

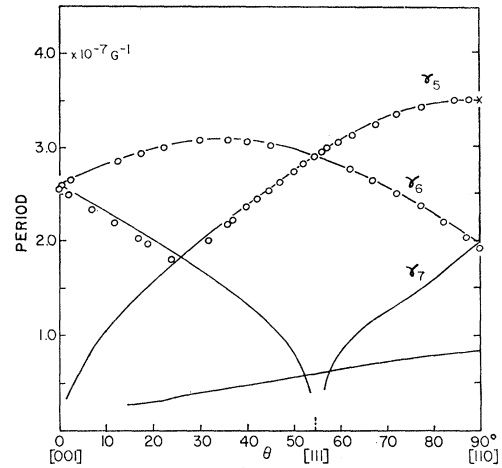


FIG. 9. The angular variation of the γ periods for the (110) plane. The period branches are labeled to be consistent with the orbits shown in Fig. 6.

ment of nearly-free-electron predictions with the ultrasonic attenuation results of Kamm and Bohm¹⁹ for the second- and third-zone surface, with Priestley's dHvA results¹⁰ for the second-zone surface, and with many features of the dHvA data for the third zone bears out this conclusion. However, such important details as the connectivity near the points W in the zone are quite sensitive to small energy differences. This severely limits the usefulness of complete band-structure calculations for predicting such behavior. Ashcroft,⁸ in his 4 OPW calculation illustrates this sensitivity to small energy difference by considering various combinations of the Fourier coefficients of the pseudopotential, V_{111} and V_{200} , and the resultant connectivity of the Fermi surface near W .

Among the several models considered by Ashcroft, only one was consistent with both HF and LF dHvA

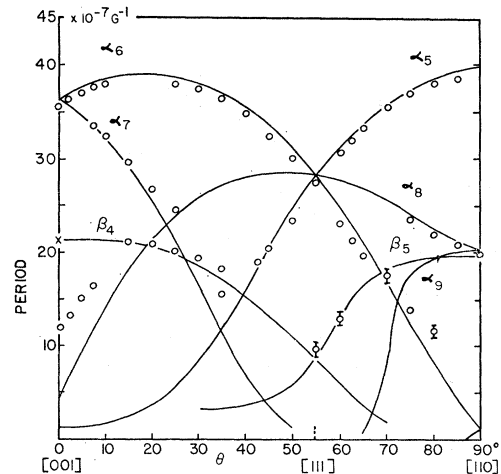


FIG. 10. The angular variation of the α and β periods for the (110) plane. The period branches are labeled to be consistent with the orbits shown in Fig. 6.

¹⁹ G. N. Kamm and H. V. Bohm, Phys. Rev. **131**, 111 (1963).

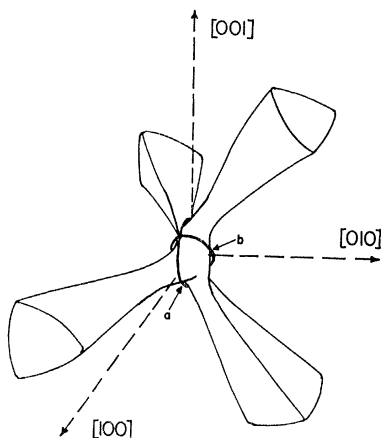


FIG. 11. An enlarged section of the third-zone Fermi surface of aluminum near the point W for Harrison's model (2) in the reduced zone scheme. The junction orbits are labeled a and b .

data of Gunnerson.⁴ This model resulted from setting V_{111} and V_{200} equal to 0.0179 and 0.0562 Ry, respectively, and is designated as model 1. Figure 4 shows model 1 for the third zone in the reduced zone scheme. An enlarged section of the Fermi surface near the point W is shown in Figs. 5 and 6. The positions of the HF and LF extremal orbits are shown in these figures. The c orbits in Ashcroft's notation are labeled β here. It should be noted that the arms join in pairs near the point W to form rings. The fact that the rings do not join each other at W gives rise to the β orbits which distinguish this model from the others. The angular variation of the dHvA periods predicted for model 1 is shown, along with the experimental data of the present work in Figs. 7–10. The agreement is very good and the few minor deviations will be discussed later.

Model 2 in Ashcroft's notation corresponds to Harrison's model^{3,5} and does not give a good fit to all of the data. A section of the Fermi surface near the point W for this model, displaying the extremal junction orbits, is shown in Fig. 11. Analysis of model 2 shows that it contains no periods whose angular variation corresponds to the experimental data points which fit closely the β orbits of Ashcroft's model 1. An extensive study (by Ashcroft) of the possible V_{111} and V_{200} values consistent with this model failed to produce a good fit to the dHvA data. In particular it was found that the values suggested by Harrison⁵ ($V_{111} = 0.0295$ Ry and $V_{200} = 0.0550$ Ry) gave poor agreement with the data. The agreement was found to improve as V_{111} and V_{200} were changed in the direction of model 1.

EXPERIMENTAL RESULTS AND DISCUSSION

Periods

Two crystal suspensions are reported here: the $\langle 100 \rangle$ and $\langle 110 \rangle$ directions vertical. The vertical rotation axis of

the electromagnet thus made it possible to study any direction in either the (100) or (110) planes. Three groups of dHvA periods were observed in this investigation and will be referred to as α , β , and γ . Figures 5 and 6 show the portions of Ashcroft's model of the third-zone Fermi surface from which these groups originate. The orbits labeled γ are associated with the thick portions of the arms while those labeled α and β are associated with necks and joints of these arms. In discussing these periods and their comparison to Ashcroft's predictions, we consider first the highest frequency group γ .

In Fig. 5, orbits γ_1 , γ_2 , and γ_3 enclose the arm cross-sectional areas observed when the magnetic field is applied in the $\theta = 0$ or $[010]$ direction. The periods corresponding to these cross sections are labeled in Fig. 7. In Fig. 6, orbits γ_5 , γ_6 , and γ_7 enclose the arm cross-sectional areas observed when the field is in the $[110]$ direction. The periods corresponding to these cross sections are labeled in Fig. 9. The cross sections defined by γ_1 , γ_2 , γ_3 , γ_6 , and γ_7 approach the common area of 0.0372 \AA^{-2} (units of reciprocal angstroms squared) in the $[100]$ direction. Those defined by γ_2 , γ_4 , γ_6 , and γ_7 approach the value 0.0498 \AA^{-2} in the $[110]$ direction. The principal third-zone arm section is defined by a (110) plane passing through the points K or U . This extremal cross section, enclosed by orbit γ_5 , is observed when the field is in the $[110]$ direction, and is found to have an area of 0.0273 \AA^{-2} . The agreement of the γ periods with this model is very good for all angles in both the (100) and (110) planes.²⁰

The possible α and β orbits for the (100) plane are shown in Fig. 5 for a field direction given by $\theta = 0$, and the corresponding periods are labeled in Fig. 8. The principal joint cross section is defined by a (100) plane passing through the point W , and is enclosed by either orbit β_1 or β_2 as shown in Fig. 5. The area of this cross section was measured to be 0.00445 \AA^{-2} . The principal cross section of the neck is given by the minimum area measured for it and is observed, at about $\theta = 25^\circ$ in the (100) plane, to be 0.00230 \AA^{-2} . In the $[110]$ direction, the β_1 and β_3 branches of the joint have the same cross section which is predicted to be about 5% larger than α_2 branch of the neck in that direction. The resolution of the present work was not sufficient to distinguish this difference. A single period, probably due to an average of these cross sections and corresponding to a cross section of 0.00483 \AA^{-2} , was observed in this region. It should be noted that in all of the above discussion, references are made to measurements taken in the $\langle 100 \rangle$ and $\langle 110 \rangle$ crystal directions. The circular data points were actually taken 0.1° to 0.5° from these directions since the torque vanishes by symmetry at

²⁰ In the vicinity of $\theta > 30^\circ$ in the (100) plane, frequency modulation effects [R. J. Higgins, J. A. Marcus, and D. H. Whitmore, Phys. Rev. **137**, A1172 (1965)] appeared in the γ oscillations due to the presence of strong β oscillations but could be clearly identified by a change of stiffness of the magnetometer.

the $\langle 100 \rangle$ and $\langle 110 \rangle$ directions. However, the crosses were obtained by modulation methods and so are within 0.1° of the symmetry axes.

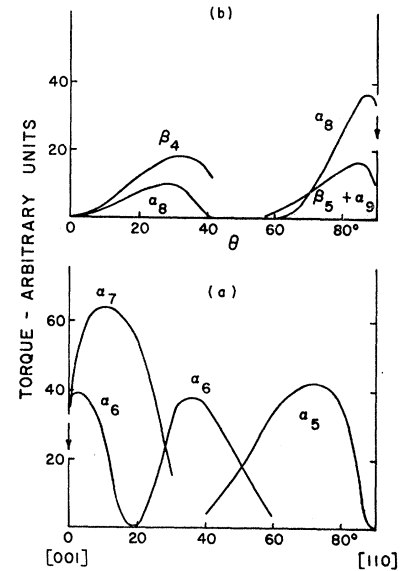
Although there are a few minor deviations from Ashcroft's model, its real test lies in the presence or absence of the β -type orbits. The two-arm joint, absent in all other proposed models, is characteristic of model 1 and results when the four arms joined at point W in Harrison's model pinch off into two pairs of arms. The two arms making up each pair meet at the joint common to both of them as shown in Figs. 4, 5, and 6.

Much experimental evidence has been found to support the β orbits. In the (100) plane, Fig. 8, the orbit β_2 has been followed from $\theta=2^\circ$ to $\theta=25^\circ$. The orbit β_1 is not observed over this range of angle. This is not unexpected because of the flatness of β_1 on Ashcroft's model and the dependence of the dHvA amplitude on $\partial P/\partial\theta$. The orbit β_1 has been followed from $\theta=30^\circ$ to $\theta=45^\circ$. It is not possible to determine whether the data point at $\theta=25^\circ$ belongs with α_3 , β_1 , or both. The β_3 and α'_2 branches are coincident making it impossible to distinguish between them. A large amplitude signal, corresponding to their common period, is observed over the range $\theta=27^\circ$ to $\theta=38^\circ$. The amplitudes of the α'_2 and α_2 signals would be expected to be about the same over this angular range since the $\partial P/\partial\theta$ terms appearing in them are very similar. It is observed, however, that the amplitude of the α'_2 , and/or β_3 signal is much larger than that of the α_2 branch over this range. It is very likely that the large difference in amplitude observed is due to the presence of the β_3 branch, giving further evidence for the β orbits.

In the (110) plane, Fig. 10, evidence has also been obtained for the existence of β orbits. The β_4 branch has been observed with large amplitude over the region from $\theta=15^\circ$ to $\theta=35^\circ$. For $\theta < 15^\circ$ the slope, $\partial P/\partial\theta$ tends to zero resulting in a vanishing dHvA amplitude. The data point at the $[111]$ direction could also be interpreted as belonging to the β_4 branch, in which case β_4 has been observed out to $\theta=54.5^\circ$. The β_5 branch is most difficult to resolve because of its nearness to the α_8 and α_9 branches and its small $\partial P/\partial\theta$ (from $\theta=75^\circ$ to $\theta=90^\circ$) but evidence has been obtained for it at $\theta=60^\circ$. It cannot be determined whether the data point at $\theta=70^\circ$ belongs with the α_6 or β_5 branch. The data point at $\theta=54.5^\circ$ must go with either (or both) the β_4 or β_5 branch and in either case is further evidence for the β -type orbits.

Having discussed the general features of the data and the agreement with Ashcroft's model, we now consider the relative amplitudes of some of the periods and the use of filters in data analysis. Considering first the longer periods in both suspensions, the 35.8×10^{-7} G $^{-1}$ periods ($\alpha_{6,7}$) are dominant in the $\langle 100 \rangle$ directions. As the field is rotated from the $\langle 100 \rangle$ direction toward the $\langle 110 \rangle$ direction, the dominance shifts gradually

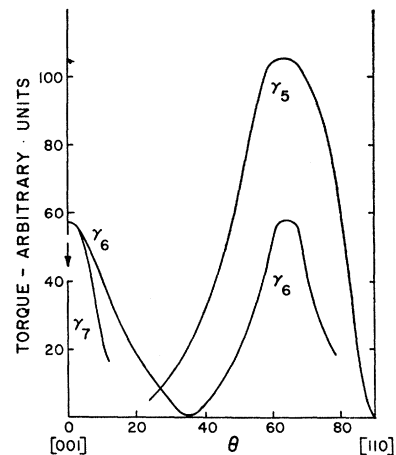
FIG. 12. Angular dependence of the α and β oscillation amplitudes for a (110) plane. Peak-to-peak values are shown for a magnetic field of 20 kG and a temperature of 4.2°K. Uncertainties are approximately $\pm 20\%$ except where periods have close values such as for α_8 , β_5 , and α_9 near $[110]$ where the separation of amplitudes is only estimated. Vertical arrows at symmetry axes indicate an abrupt drop in amplitude due to phase cancellation.



until in the $\langle 110 \rangle$ direction, the 19.8×10^{-7} G $^{-1}$ period is heavily dominant. Figure 12 illustrates this variation of the torque amplitude for the $[110]$ suspension. While these curves are not based on a careful separation of relative amplitudes, they are indicative of the general angular dependence. The amplitudes of the γ group are similarly sketched in Fig. 13 for the $[110]$ suspension. Observation at higher magnetic field or lower temperature enhances the oscillations with larger cyclotron mass relative to those of smaller mass. The torque amplitude vanishes at $\langle 100 \rangle$ and $\langle 110 \rangle$ axes as symmetry requires, dropping slowly for those branches whose $\partial P/\partial\theta$ vanishes at these axes and very abruptly due to phase cancellation for branches with finite $\partial P/\partial\theta$.

In angular regions where a single period is clearly dominant, a simple counting procedure is adequate for computing the period between known field values. In regions where several periods were observed to have

FIG. 13. Angular dependence of the γ oscillation amplitudes for a (110) plane. Torques in Figs. 12 and 13 can be found from the calibration that 20 units correspond to 1.3 dyn cm. Since the crystal weighed 0.045 g, 20 units also correspond to a peak-to-peak susceptibility oscillation of 7.2×10^{-9} cgs units/g.



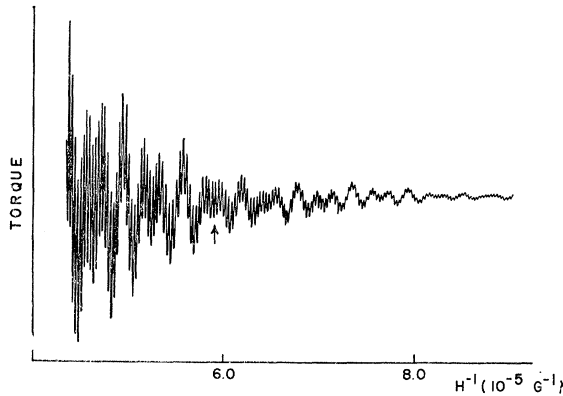


FIG. 14. The unfiltered data taken at 4.2°K for $\theta=25^\circ$ in the (100) plane. α , β , and γ periods are present. The arrow indicates the field position at which the sweep shown in Fig. 15 begins.

comparable amplitudes it was necessary to filter out certain components before analysis based on a clear beat pattern could be done. Where it was only desired to separate the γ from α and β periods the broad band ($Q=0.6$) filter was used. These periods differ by about a factor of 10 and are easily separated. Although it would appear nonessential to filter out components differing by a factor of 10 it is, in fact, useful for two reasons. First of all, the counting accuracy is improved by getting rid of wave distortions due to the unwanted component, and secondly, many smaller amplitude components were discovered in this manner.

The problem of resolving the several α and β frequencies was more difficult, however, and required the use of a narrow band filter ($Q\approx 3$). The effect of filtering with a $Q\approx 3$ filter can best be illustrated by the following examples. At $\theta=10^\circ$ in the (100) plane three long periods are observed. The α_1 and α_3 periods ($30.7\times 10^{-7} \text{ G}^{-1}$ and $38.7\times 10^{-7} \text{ G}^{-1}$, Fig. 8) are of comparable amplitude and are heavily dominant. The $21.0\times 10^{-7} \text{ G}^{-1}$ period, corresponding to an average between the β_2 branch of the joint and the α_4 branch of the neck which are too nearly equal in period to be resolved, can only be determined if the filter is set at maximum gain for this period. In this situation, the $21.0\times 10^{-7} \text{ G}^{-1}$ period becomes dominant and beats primarily with the $30.9\times 10^{-7} \text{ G}^{-1}$ period while the γ oscillations are reduced in amplitude by more than a factor of 100.

A second illustration shows the use of the narrow band filter to identify frequency components which otherwise could not be resolved. Figure 14 shows the unfiltered data for $\theta=25^\circ$ in the (100) plane while Fig. 15 illustrates data taken with the narrow band filter peaked for the $20.2\times 10^{-7} \text{ G}^{-1}$ period. The data curve shown in Fig. 15 begins at the field position indicated by the arrow in Fig. 14 and the sweep rate is the same. In this pattern the 11:12 beat corresponds to the β_1 and/or α_3 branch beating with the dominant β_2 branch. The 2:3 beat corresponds to the α_2 and/or α_4 branch beating with the β_2 branch.

In the situations where beat analysis of two periods was necessary the carrier, or dominant frequency, was first determined by direct counting and the other period was then calculated using a standard beat analysis. It was determined whether the carrier was the higher or lower frequency of the two by investigating the beat waist. If the carrier was spread in the waist it was assumed that the carrier was the lower frequency while if it was contracted it was assumed to be the higher. This procedure has been discussed in greater detail by Joseph.²¹ Several representative data plots have been reproduced on the CSI analog computer available and have proven this method of analysis to be reliable. If the data contain three components, this technique can only be used if one is strongly dominant such as in the case illustrated in Fig. 15. The filters were often useful for making the desired component dominant.

When the filters were used the periods were calculated using a wavelength analysis. The time drive was calibrated in G^{-1} making it possible to measure the length of several oscillations directly from the data sweep. The measured length was then converted to reciprocal gauss giving the $\Delta(1/H)$ interval necessary to determine the period of oscillation.

Volskii,⁹ observing quantum oscillations in the high-frequency surface resistance of aluminum, has also measured the α , β , and γ periods in the (100) and (110) planes. The results of this work are found to be in excellent agreement with Volskii. He does not, however, indicate evidence for the "neck" branch labeled α_4 in the (100) plane (Fig. 8) and α_8 in the (110) plane (Fig. 10) which were observed in this work. Additional evidence has also been obtained, in this work, for the γ_4 and α_2 branches in the (100) plane, and the β_5 branch in the (110) plane.

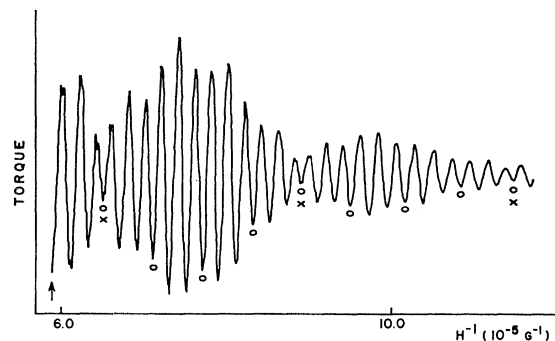


FIG. 15. The dHvA data taken at 4.2°K for $\theta=25^\circ$ in the (100) plane after narrow band filtering to remove the γ component. There are two types of beats present after peaking the filter for the $20.2\times 10^{-7} \text{ G}^{-1}$ period. The waists of the 3:2 beat are labeled \circ and the waists of the 12:11 beat are labeled \times . The arrow indicates the field position labeled by an arrow in Fig. 14 and the sweep rates are identical.

²¹ A. S. Joseph, thesis, Case Institute of Technology, 1962 (unpublished).

In summary, then, the comparison of the predictions of Ashcroft's model 1 with the experimental data shows generally excellent agreement with a few minor deviations. One of these cases arises near the $\langle 100 \rangle$ direction where the period labeled α_4 in the (100) plane and α_8 in the (110) plane is observed to be larger than predicted by Ashcroft. This period corresponds to the orbit labeled α_4 in Fig. 5. The fact that the area is measured to be smaller than predicted indicates that the neck probably extends further up the arm than indicated by Ashcroft. This lengthening of the neck is consistent with a slight broadening of the arm-neck transition region as indicated by the γ_8 branch in which the experimental points drop below the predicted curves. The α_1 , α_2 , and α_3 branches of the neck have the common measured period of $35.8 \times 10^{-7} \text{ G}^{-1}$ in the $\langle 100 \rangle$ direction as compared to the value of $36.3 \times 10^{-7} \text{ G}^{-1}$ measured by Gunnerson⁴ and used by Ashcroft⁸ to help determine V_{111} and V_{200} . These discrepancies are very slight and it must be concluded that Ashcroft's model is in excellent agreement with the results of this work.

Cyclotron Masses and Dingle Temperatures

In orientations where it could be determined, the temperature dependence of the amplitude of the torque oscillations was measured and used to determine the effective cyclotron masses. Lifshitz and Kosevitch² have shown that, for a given crystal orientation, the amplitude A of the torque oscillations can be expressed as

$$A = A_0 H^{1/2} T \exp[-\xi \eta (T+x)],$$

where A_0 is a constant depending upon the orientation of H relative to the crystalline axes, $\xi \equiv 2\pi^2 kmc / e\hbar H$, $\eta \equiv m^*/m$, and x is the Dingle²² temperature which takes into account the broadening of the energy levels due to collisions. One assumption made here is that an expression, $1 - \exp(-2\xi\eta T)$, which should appear in the denominator, can be replaced by unity. This assumption results in an error of about 1% in the most extreme cases which arise in aluminum for the range of magnetic fields used in this determination of masses. Using this expression for the amplitude, the following expression can be written for the effective mass ratio η :

$$\eta = -(e\hbar H / 2\pi^2 kmc) S,$$

where S is the slope of the plot of $\ln(A/T)$ as a function of T at the constant field H . All quantities are expressed in Gaussian units. The above amplitude expression also yields the following expression for the Dingle temperature x :

$$x = -(e\hbar / 2\pi^2 m\eta c) S' - T,$$

where S' is the slope of the plot of $\ln(A/H^{1/2})$ as a function of $1/H$ at the constant temperature T .

The pressure at the liquid-helium surface was controlled and measured to 0.5 mm of Hg. The mass data were taken by fixing the orientation and plotting the torque as a function of $1/H$ for several temperatures ranging from 4.2°K down to 1.85°K. The amplitude of the oscillations is orientation-dependent so the masses were taken in one field position per pump down to avoid having to reset the field position. In the $\langle 100 \rangle$ and $\langle 110 \rangle$ directions, where only one of each of the long and short periods were present, their masses were easily determined, but in orientations where several of each type were present filtering was necessary. When filtering is necessary and the amplitude of the oscillation is desired, extreme care must be taken to ensure that the torque corresponding to a given field value occurs at the same filter gain value for each temperature. The slight imperfections in the $1/H$ drive result in a frequency of oscillation which is not quite constant in time. The narrow band filter has a gain-frequency curve which is steeply peaked at the tuned frequency. The small variations in frequency for a given oscillation due to $1/H$ drive variations are therefore observed as variations in amplitude. Since only the slope of the $\ln(A/T)$ versus T plot is needed to determine an effective cyclotron mass, an absolute amplitude is not required, and it is only necessary that the $1/H$ drive be accurately reproducible from sweep to sweep. If the Dingle temperature is desired, however, the amplitude as a function of field, for a fixed sample temperature, must be determined. This can be accurately done only when one or two frequency components are present. One assumes that mosaic structure in the crystal does not produce long beat patterns which would yield a spurious field dependence. Dingle temperatures were not determined for orientations where narrow band filtering was required, since the accurate amplitude analysis required became prohibitively tedious and uncertain.

In determining masses, the broad band filter was used to separate the long and short periods. If more than two similar periods remained after this filtering procedure, the narrow band filter was then used. Mass data were only taken in orientations where the number of periods present with large amplitude could be reduced to one or, at most, two. In orientations where it was necessary to work with two periods it was possible to use a beat analysis to arrive at the amplitudes of the component periods. For the case of symmetric beats, the antinodes in the pattern correspond to the sum of the two component amplitudes, $A+B$, while the nodes correspond to their difference, $A-B$, thus yielding two equations for determining the two unknown component amplitudes, A and B . The field position to be used was chosen at a node and the appropriate $A+B$ value for this field determined by interpolation between neighboring antinodes. This procedure was repeated at the same field position for each

²² R. B. Dingle, Proc. Roy. Soc. (London) **A211**, 517 (1952).

TABLE I. γ -orbit masses.

θ^a	$P(10^{-7} \text{ G}^{-1})$	dHvA	m^*/m Cycl. res. ^b	Band str. ^c	$\frac{m^*_{\text{obs}}}{m^*_{\text{BS}}}$	$\frac{(m^*/m)P}{(10^{-7} \text{ G}^{-1})}$ Cycl. res.
(001) Plane						
0.1	2.57	0.180±0.004		0.136	1.32	0.436
5.0	2.75	0.165±0.004				0.454
25.0	3.32	0.137±0.005				0.455
	2.40	0.191±0.005				0.458
40.0	3.48	0.131±0.003				0.456
44.9	1.97	0.227±0.005				0.447
45.0	3.50	0.130±0.004 ^d		0.095	1.37	0.455
(110) Plane						
0.1	2.57	0.180±0.004	0.183	0.136	1.32	0.463
10.0	2.82	0.163±0.004	0.168			0.460
35.0	2.11	0.21±0.010	0.222			0.444
54.5	2.90	0.150±0.006	0.161			0.435
62.5	2.75	0.160±0.008	0.170			0.440
89.9	1.97	0.227±0.004	0.233			0.447

^a θ is measured in degrees from a (100) direction.

^b See Ref. 11.

^c See Refs. 8 and 12 for data in Tables I and II.

^d Extrapolated from $\theta=40^\circ$ point assuming a $\cos\theta$ dependence over this small angular range.

temperature and the resulting $\ln(A/T)$ and $\ln(B/T)$ values were plotted to obtain the slope needed in the above expression for η . This expression was then used to determine the mass ratio for each of the two components, A and B .

Dingle temperatures were determined in only two field orientations, $\theta=5^\circ$ in the (100) plane, and $\theta=54.5^\circ$ in the (110) plane. At $\theta=5^\circ$ in the (100) plane, the broad band filter was used to remove the α component. The result was a uniform beat pattern between the two γ periods 2.37 and $2.75 \times 10^{-7} \text{ G}^{-1}$. From the average of the values of $\ln[(A+B)/H^{1/2}]$ and $\ln[(A-B)/H^{1/2}]$ versus H^{-1} the Dingle temperature for the dominant oscillation ($2.75 \times 10^{-7} \text{ G}^{-1}$) was determined to be $0.9 \pm 0.2^\circ \text{K}$. At $\theta=54.5^\circ$ in the (110) plane no filtering was required and the Dingle temperature was determined for the $2.89 \times 10^{-7} \text{ G}^{-1}$ period. Much care was taken in setting the field along the [111] axis to avoid a long beat due to slight misorientation. The Dingle temperature in this orientation was found to be $0.8 \pm 0.2^\circ \text{K}$.

The Dingle temperature x can be expressed as a collision time τ through the expression²²

$$x = \hbar / 4\pi^2 k \tau.$$

The Dingle temperature of 0.8 mentioned above for $\theta=54.5^\circ$, corresponds to orbits of the type γ_5 and γ_6 and yields a collision time of 1.6×10^{-12} sec. Using a field of 20 kG and the appropriate cyclotron mass, this τ yields an $\omega_c \tau$ of 3.6. For comparison to cyclotron resonance experiments at 2 kG where the fundamental resonance should occur for a frequency of 35 GHz used by Moore and Spong,¹¹ $\omega_c \tau$ is approximately 0.36 for our samples. Although the samples used in this work have a lower resistance ratio (5000 compared with 10 000) than those of Moore and Spong,¹¹ it is not surprising that difficulties are encountered when at-

tempts are made to observe subharmonic series in the cyclotron resonance experiments.

Cyclotron mass data have been obtained in representative field orientations for both the (100) and (110) suspensions and are listed in Tables I and II, as reported earlier,²³ along with the oscillation periods to which they correspond. In estimating uncertainties, a factor of 2 (in Table I) and 3 (in Table II) times the scatter of the individual values obtained at a given orientation has been arbitrarily introduced to allow for small systematic errors except where clear beating of several components occurred. In these cases, uncertainties are quite difficult to estimate, even for two-component beats, because of the sensitivity to relative amplitude and phase in nodes and antinodes. Even if there is a marked difference in relative amplitude, the mass of the dominant oscillation appears to be shifted slightly in the direction of the other mass and vice versa. Along symmetry directions where the beat structure is much less complicated, our results should be more reliable. This is borne out in the γ group by comparison to the cyclotron resonance data as illustrated in Table I where the agreement is good at [001] and [110] but unexpectedly low at [111] ($\theta=54.5^\circ$). This discrepancy near [111] will be discussed later.

The cyclotron resonance data of Moore and Spong¹¹ were chosen for this comparison because of the accuracy and clear identification provided by their ob-

TABLE II. α - and β -orbit masses.

θ^a	$P(10^{-7} \text{ G}^{-1})$	dHvA	Band str.	$\frac{m^*_{\text{obs}}}{m^*_{\text{BS}}}$	$\frac{(m^*/m)P}{(10^{-7} \text{ G}^{-1})}$ dHvA
(001) Plane					
0.0	21.3 β	0.102±0.006	0.066 β	1.55	2.18
0.5	35.5 α	0.091±0.003	0.0605 α	1.50	3.23
19.5	26.4 α	0.121±0.004			3.19
	20.7 β	0.090±0.004			1.86
25.0	20.3 β	0.096±0.004			1.95
	30.1 α	0.103±0.004			3.10
38.0	20.9 β	0.100±0.004			2.09
	18.4	0.115±0.004			2.12
44.9	19.8	0.118±0.003 ^b	0.074 β		2.34
(110) Plane					
0.0	21.3 β	0.102±0.006	0.066 β	1.55	2.17
0.5	35.5 α	0.091±0.004	0.0605 α	1.50	3.23
9.5	37.9 α	0.090±0.004			3.41
	32.7 α	0.100±0.004			3.27
45.0	32.5 α	0.108±0.004			3.51
	20.3 α	0.136±0.005			2.76
62.5	32.0 α	0.112±0.005			3.58
	21.3 α	0.139±0.006			2.96
70.0	35.5 α	0.091±0.004			3.23
89.9	19.8	0.119±0.003 ^b	0.074 β		2.34

^a θ is measured in degrees from a (100) direction. Obtained by field-modulation technique.

^b This mass may arise from a combination of α - and β -orbit masses whose values may be estimated as 0.16 and 0.10, respectively, from the appropriate $(m^*/m)P$ products. This assumption yields a ratio $m^*_{\text{obs}}/m^*_{\text{BS}}$ of 1.4 for the β orbits.

²³ C. O. Larson and W. L. Gordon, Phys. Letters 15, 121 (1965).

servation of several subharmonics of each mass resonance. They measured the γ masses in the (110) plane to an accuracy of 1% but, unfortunately, were unable to reliably identify masses corresponding to the α or β groups. The dHvA masses for the γ group in the (110) plane, as determined in this work, are consistently lower than the cyclotron resonance masses except at the [100] and [110] directions where they agree almost exactly. In an effort to make the most accurate comparison possible in this plane, the [111] direction mass was chosen for careful study. In this orientation only the $2.89 \times 10^{-7} \text{ G}^{-1}$ (γ) and the $27.5 \times 10^{-7} \text{ G}^{-1}$ (α) periods were present in the data, making possible an accurate determination of the γ mass. Since the γ component was highly dominant, comprising about 96% of the total amplitude, no filtering was required. However, it was found that there was a slight interaction between the measured γ amplitudes and the α oscillations, in spite of the frequency ratio of approximately 10:1. This small effect was averaged out by determining the γ mass at sufficient field positions to span several α periods. In such measurements near symmetry axes, the strong angular dependence of the amplitude can produce systematic errors. The precaution of maintaining a fixed magnet position during a temperature run for each of the orientations at which the mass was determined should have been adequate to rule out this error.

The more recent data of Galkin *et al.*²⁴ are not included in this comparison of dHvA and cyclotron resonance masses since their data show no subharmonic resonances for the masses discussed here. One of their families of masses, labeled κ , requires special mention, however. They attribute these masses to orbits around a junction of four necks as predicted by Harrison's model. Junction orbits of this type are inconsistent with the presence of β orbits, predicted by Ashcroft, and observed in this work and that of Volskii.⁹ It is not clear just what part of the Fermi surface would yield a mass family having the angular dependence exhibited by κ . In the (100) plane they could possibly correspond to a branch of the arm periods having the value $1.95 \times 10^{-7} \text{ G}^{-1}$ in the [110] direction and labeled γ_4 in Fig. 7. The mass plot corresponding to this branch of periods would be expected to increase in somewhat the manner they observed in the (100) plane as θ is decreased in sweeping away from a $\langle 110 \rangle$ direction. It would be expected, however, that this branch of masses would also increase for θ decreasing from the [110] direction in the (110) plane. The data of Galkin *et al.*²⁴ however, are found to decrease in this range, casting doubt on this interpretation.

In orientations where the dHvA periods and the corresponding cyclotron masses have both been de-

termined, it is interesting to examine the product $(m^*/m)P$. A sufficient condition for the product of band-structure mass and period to remain constant with angle is that the extremal area of a given portion of the Fermi surface may be described as a separable function of angle and energy.²⁵ If the enhancement of the band-structure mass, discussed at the end of this section, is isotropic over this portion of the Fermi surface the measured cyclotron mass can provide an equally useful comparison. This comparison is shown in the final columns of Tables I and II. Within experimental uncertainties, the results of this work yield for the γ group, shown in Table I, a constant product in the (100) plane having a mean value of $0.46 \times 10^{-7} \text{ G}^{-1}$. This is not true in the (110) plane, however, where the dHvA products show deviations of as much as 6% below this value. If the cyclotron resonance¹¹ masses are used with the dHvA periods, however, the $(m^*/m)P$ product remains nearly constant. This is not unexpected since the cyclotron resonance masses in the HF group lie close to those expected for a cylindrical surface out to 50° or more from the cylinder axis in the (110) plane.

Cyclotron resonance experiments measure extremal masses whereas dHvA experiments measure extremal areas. In all simple cases considered it would seem that these should define the same orbit and therefore the same mass. It has been pointed out by Spong and Kip²⁶ that the cyclotron resonance experiments generally observe slightly broader orbits which can be made up of orbits differing in mass by approximately 1%. This would serve to raise or lower the mass measured depending upon whether a minimum or maximum was observed. Such effects are not expected to be important for the γ orbits involved here so that where a discrepancy exists it is probably due to systematic errors in the present data.

The longer period data are shown in Table II. Here the mass-period products seem to group around the two distinct values, 3.2 and $2.0 \times 10^{-7} \text{ G}^{-1}$ for the α and β orbits, respectively. At $\theta = 45^\circ$ and 62.5° in the (110) plane, where the α products seem to diminish for orbits α_5 and α_6 , respectively, beats are present in the dHvA oscillations. The presence of beats makes it difficult to determine whether this represents a trend toward a decreasing product as orbits approach neck junctions, or is a result of increased uncertainties in the mass data. Reproduction of the 45° data on the analog computer would tend to indicate the former. An unusual situation arises at $\langle 110 \rangle$ where in both the (100) and (110) planes an intermediate product 2.36×10^{-7}

²⁴ A. A. Galkin, V. P. Naberezhnykh, and V. L. Mel'nik, *Fiz. Tverd. Tela* **5**, 201 (1963) [English transl.: *Soviet Phys.—Solid State* **5**, 145 (1963)].

²⁵ If the extremal cross section $S_m = U(E)V(\theta)$, then $(m^*/m)P \propto U'/U$ follows from the relations $P \propto 1/S_m$ and $(m^*/m) \propto \partial S_m / \partial E$. Thus, $(m^*/m)P$ should be constant, independent of angle for a given portion of the Fermi surface which scales with energy without change of shape. This condition is satisfied by quadratic energy bands where the product is proportional to E_F^{-1} as measured from the bottom of the band.

²⁶ F. W. Spong and A. F. Kip, *Phys. Rev.* **137**, A431 (1965).

G^{-1} appears. In the (100) plane this could be the result of a weighted mean of α and β orbits since in this plane both have fairly strong amplitudes of oscillation near $\langle 110 \rangle$, and according to Ashcroft's model, arise from separate orbits. Assuming the mass-period products for α and β orbits to be 3.2 and $2.0 \times 10^{-7} G^{-1}$, respectively, separate masses of approximately 0.16 and 0.10 can be obtained for these orbits. This reduces the ratio $m_{\text{obs}}^*/m_{\text{BS}}^*$ to 1.4 for the β orbit, a value more consistent with the idea of a constant mass-period product and with the results of Volskii as reported by Ashcroft.¹²

This explanation of the intermediate product seems less likely in the (110) plane where, although the orbits remain separate, the oscillation amplitude from the β orbits should vanish near $\langle 110 \rangle$ for torque measurements since $\partial A/\partial \theta$ tends to zero. Thus, the mass measured for $\langle 110 \rangle$ in this plane would be expected to reflect the 0.16 mass value estimated above for the α -orbits. Instead, the observed mass is identical to that found in the (100) plane. A possible explanation lies in the assumption that the torque measurements yield only α orbits at $\langle 110 \rangle$ in both planes and that the intermediate mass-period product corresponds to a decreasing value for the α orbits as they approach a common value with the β orbits ($\alpha_2 \rightarrow \alpha_2'$, β_3 in Fig. 8). If this assumption is correct, then we are unable to obtain a value for the mass enhancement in the $\langle 110 \rangle$ direction since m_{BS}^* applies only to the joint (β_3 orbit).

As mentioned above, Ashcroft and Wilkins¹³ showed that the effective mass which appears in both the electronic specific heat and the cyclotron frequency at low fields should be enhanced from its band-structure value by electron-phonon interaction. They estimate an enhancement factor of 1.48. Wilkins and Woo²⁷ have recently pointed out that the cyclotron mass appearing in the temperature-dependent amplitude of the dHvA oscillations is also enhanced by these interactions. Thus, it is not surprising that the cyclotron masses reported here are in general agreement with the results of cyclotron resonance and that enhancement factors [$m_{\text{obs}}^*/m_{\text{BS}}^*$ of Tables I and II] for the symmetry directions in which band-structure masses^{8,12} are available lie between 1.3 and 1.5. These results for orbits on the third-zone portion of the Fermi surface seem to indicate that the enhancement factor is consistently lower for the γ orbits than for the α and β orbits on the assumption that only α orbits participate at $\langle 110 \rangle$. If that mass is actually due to a combination of α and β orbits, then the difference becomes much less pronounced (see footnote to Table II).

Therefore, while there may be anisotropy in the enhancement factor over the third-zone surface, there are enough combined uncertainties in observed and predicted masses to allow just as convincing an argument for isotropy. For the present, then, we can only

conclude that, isotropic or not, the enhancement factor lies within $\pm 15\%$ of the calculated value of 1.48.¹³

SUMMARY

The dHvA measurements of this investigation are consistent with the model of the third-zone Fermi surface of aluminum as proposed by Ashcroft. The junction periods observed have been found to be inconsistent with the nearly-free-electron model due to Harrison.

Two distinct classes of dHvA periods have been observed for both the (100) and (110) suspensions. The shorter periods have been attributed to the third-zone arm section (γ) as first suggested by Harrison, while the longer periods have been assigned to the neck (α) and joint (β) sections as proposed by Ashcroft. Strong experimental evidence has been found for the existence of these β orbits which are characteristic of Ashcroft's model.

Cyclotron masses have been determined in representative field orientations and are found to be in reasonable agreement with the cyclotron resonance results of Moore and Spong. A slight discrepancy has been observed, however, between cyclotron masses as measured by dHvA and cyclotron resonance techniques in some orientations. In the (110) plane the dHvA masses were measured to be as much as 6% lower than the corresponding cyclotron resonance masses except at the $\langle 100 \rangle$ and $\langle 110 \rangle$ symmetry directions, where agreement was excellent. This discrepancy may well lie within the systematic error of the present dHvA measurements and indicates the need for a more satisfactory method of separating the individual oscillation amplitudes.

Representative mass-period products have been calculated for the α , β , and γ families of orbits. The products have been found to be nearly constant for each of these three families over limited ranges in angle. The range in angle, as well as the value of the constant, depends upon the family under consideration. The range extended over the entire (100) and (110) planes for the nearly-free-electron-like arms γ , as would be expected, but was more limited for the α and β orbits. A sufficient condition for the product of band-structure mass and period to remain constant with angle is that the extremal area of the corresponding portion of the Fermi surface may be written as a separable function of angle and energy.

In orientations where theoretical band-structure masses were available, the ratio of the observed dHvA mass to the band-structure mass has been determined. This ratio for the γ orbits was found to be 1.32 in a $\langle 100 \rangle$ direction and 1.37 in a $\langle 110 \rangle$ direction. For the α orbits it was found to be 1.50 in a $\langle 100 \rangle$ direction and for the β orbits it was found to be 1.55 in a $\langle 100 \rangle$ direction and possibly 1.40 in the $\langle 110 \rangle$ direction. This ratio gives a measure of the enhancement of the band-

²⁷ J. W. Wilkins and J. W. F. Woo, Phys. Letters 17, 89 (1965).

structure mass due to the electron-phonon interaction according to Ashcroft and Wilkins¹³ who calculated an enhancement factor of 1.48 for aluminum. Uncertainties in the calculated and observed masses make it impossible to determine whether or not the enhancement is isotropic over the entire third-zone surface. It can be concluded, however, that the enhancement factor does not vary by more than $\pm 15\%$ of the calculated value.

ACKNOWLEDGMENTS

The authors have benefited from many enlightening conversations with Professor J. P. G. Shepherd, Professor P. L. Taylor, and Professor T. G. Eck. Professor W. A. Harrison and Professor N. W. Ashcroft have been helpful in discussing their work with us. We acknowledge also the cooperation of the Case Systems Research Center in making their CSI-analog computer available for data analysis.

Survey of Thermal-Neutron Damage in Pure Metals*

R. R. COLTMAN, C. E. KLABUNDE, AND J. K. REDMAN

Solid State Division, Oak Ridge National Laboratory, Oak Ridge, Tennessee

(Received 3 October 1966)

Data are presented on the production and subsequent isochronal annealing behavior of thermal-neutron damage in 14 high-purity metallic elements. Values are obtained for the specific resistivity $\delta\rho_D$ associated with the damage produced by neutron capture at 3.6°K. Comparison between experimental damage-production results and simple displacement theory is made for some elements. Comparisons are made between the recovery behavior of the various metals, as well as comparisons with other damage-production methods.

INTRODUCTION

UPON capture of a thermal neutron the nucleus of an atom emits a characteristic spectrum of γ rays as it returns from a more to a less excited or stable state. For most elements the total emitted γ -ray energy per capture is about 7–10 MeV, and the event takes place in about 10^{-14} sec after neutron capture. In metals the γ -ray emission can cause many types of atoms to recoil with sufficient energy to produce one or more Frenkel pairs. To a certain extent thermal-neutron damage is unique in that its nature is determined by the combined lattice and nuclear properties of the element, and not by the energy of incoming radiation. This report is intended to serve several purposes:

- (1) To present a characterization of the production and recovery of thermal-neutron damage in several metallic elements.
- (2) To provide a survey of the behavior of damage in those elements which have received little or no attention elsewhere.
- (3) Where possible, to provide a comparison of the behavior of thermal-neutron damage with damage produced by other mechanisms.

Previous work¹ on thermal-neutron damage reported the isochronal recovery from 4.5 to 70°K for four elements. The present work extends the number of ele-

ments and the isochronal recovery study from 3.5 to 300°K. In addition, the ratio of thermal to fast-neutron flux is presently higher than the previous value. Two criteria were used in selecting the elements to be studied. First, the capture cross section of the element must be large enough to obtain resistance changes which can be studied with reasonable accuracy. Second, the element must be pure enough so that recovery results are not grossly affected by the presence of impurities.

SPECIMEN PREPARATION

All specimens were in the form of polycrystalline wires except cadmium which was a polycrystalline ribbon and tungsten which was a single-crystal rod. It is known² that the residual resistivity of high-purity copper can be considerably reduced by annealing in the presence of a small amount of air. It is thought that the scattering cross sections of some impurities are substantially lowered by internal oxidation. The possibility is also recognized that the mechanism of internal oxidation might lead to the growth of impurity-oxide precipitates, thus further lowering the residual resistivity. In an attempt to improve the accuracy of the radiation damage resistance measurements by lowering the residual resistivity, several of the elements were given various internal oxidation treatments. It was found that these treatments also reduce the residual

* Research sponsored by the U. S. Atomic Energy Commission under contract with Union Carbide Corporation.

¹ R. R. Coltman, C. E. Klabunde, D. L. McDonald, and J. K. Redman, *J. Appl. Phys.* **33**, 3509 (1962).

² R. R. Coltman, T. H. Blewitt, and S. T. Sekula, *Nouvelles Propriétés Physiques et Chimiques des Métaux de Très Haute Pureté* (Centre National de la Recherche Scientifique, Paris, 1959).